

Review

# Elastic and damping characterizations of acoustical porous materials: Available experimental methods and applications to a melamine foam

Luc Jaouen<sup>a,\*</sup>, Amélie Renault<sup>b</sup>, Mickael Deverge<sup>c</sup>

<sup>a</sup> *Matelys – Acoustique & Vibrations, 20/24 rue Robert Desnos, 69 120 Vaulx-en-Velin, France*

<sup>b</sup> *LASH/DGCB (URA CNRS 1652), ENTPE, rue Maurice Audin, 69 518 Vaulx-en-Velin Cedex, France*

<sup>c</sup> *Laboratoire d'Acoustique de l'Université du Maine, UMR CNRS 6613, 72085 Le Mans Cedex, France*

Received 29 November 2006; received in revised form 30 November 2007; accepted 30 November 2007

Available online 14 January 2008

## Abstract

Acoustical porous materials like polymer foams or mineral wools are widely used in noise and vibration control. The acoustic efficiencies of these materials may be influenced by their elastic and damping properties. It is thus important to determine parameters such as Young's or shear moduli, Poisson's ratios and loss factors.

The first objective of this paper is to present a comprehensive list of current available techniques and difficulties faced in the estimations of the elastic and damping parameters for acoustical porous materials. The second objective is to apply the maximum number of these methods to the characterization of a porous material and to discuss the results.

In a first part, a brief recall of the mechanical behaviors of acoustical porous materials is given. This part includes a discussion on the influence of viscoelasticity and anisotropy often observed in porous materials. A description of experimental methods used for the elastic and damping characterizations of acoustical porous materials is also given. In total, three groups of quasistatic methods and six groups of dynamic methods are presented. Their main advantages and drawbacks are reported and discussed.

In a second part, five of the presented methods are applied to a melamine foam to investigate the frequency and temperature dependences of its elastic and damping parameters. Characterization results are compared and discussed.

© 2007 Elsevier Ltd. All rights reserved.

PACS: 46.40.Ff; 43.40.+s

Keywords: Acoustical porous materials; Elastic parameters; Characterization methods

## Contents

|   |      |
|---|------|
| 1. Introduction . . . . .   | 1130 |
| 2. Mechanical behavior . . . . .  | 1130 |
| 2.1. Viscoelasticity . . . . .  | 1130 |
| 2.2. Anisotropy and inhomogeneity . . . . .                                 | 1131 |
| 3. Descriptions of the methods . . . . .                                    | 1131 |
| 3.1. Brick under uniaxial compression loading, quasistatic regime . . . . . | 1132 |
| 3.2. Cylinder under torsion loading, quasistatic regime . . . . .           | 1132 |

\* Corresponding author.

E-mail address: [luc.jaouen@matelys.com](mailto:luc.jaouen@matelys.com) (L. Jaouen).

|      |  |      |
|------|--|------|
| 3.3. | Layer under pure shear loading, quasistatic regime . . . . .       | 1132 |
| 3.4. | Beam under longitudinal vibrations . . . . .                       | 1133 |
| 3.5. | Brick under uniaxial compression loading, dynamic regime . . . . . | 1133 |
| 3.6. | Beam under bending vibrations . . . . .                            | 1133 |
| 3.7. | Plate under bending vibrations . . . . .                           | 1134 |
| 3.8. | Acoustical excitation-based methods . . . . .                      | 1134 |
| 3.9. | Phase velocity measurement-based methods . . . . .                 | 1134 |
| 4.   | Summary and discussion . . . . .                                   | 1134 |
| 5.   | Application to a melamine foam . . . . .                           | 1135 |
| 5.1. | Brick under compression loading, quasistatic regime . . . . .      | 1136 |
| 5.2. | Cylinder under torsion loading, quasistatic regime . . . . .       | 1137 |
| 5.3. | Beam under longitudinal vibrations . . . . .                       | 1138 |
| 5.4. | Beam under bending vibrations . . . . .                            | 1138 |
| 5.5. | Plate under bending vibrations . . . . .                           | 1138 |
| 5.6. | Comparison of the results . . . . .                                | 1138 |
| 6.   | Conclusion . . . . .   | 1139 |
|      | Acknowledgements . . . . .   | 1139 |
|      | References . . . . .   | 1139 |

## 1. Introduction

In the past few years, numerous new experimental methods have been proposed to characterize the elastic and damping parameters of fibrous materials or open-cells and air saturated polymer foams.

These materials are widely used for sound absorption and insulation in buildings, inside the fuselage of airplanes, in machinery enclosures, etc. The influence of their elastic parameters (Young's or shear moduli, Poisson's ratios, loss factors, etc.) may be important when porous materials are bounded onto the vibrating structure. When backed by a rigid wall, the absorption coefficients of these materials may also be noticeably influenced at the quarter wavelength resonance and its harmonics (cf. [1], Chapter 6, Section 6).

The recent development of new methods to assess these elastic parameters denotes an actual effort to consider the mechanical and particularly viscoelastic behavior of porous materials. The knowledge of the intrinsic material parameters is crucial for quality controls or for more accurate predictions of their acoustic performances. This effort also denotes the search for a unique characterization method, or at least a limited set of methods, suitable for most of the acoustical materials.

In this context, we will list commonly used and more recent experimental methods for the determination of Young's or shear moduli, Poisson's ratios and loss factors of acoustical porous materials. The focus is put on the experimental set-ups or more precisely experimental configuration rather than on the global method used to identify the material parameters from the measurements. Most of the experimental methods described here are adaptations of techniques used for polymers or metal [4,10,22] to estimate Young's moduli and loss factors ranging from approximately  $10^3$  to  $10^7$  N m<sup>-2</sup> and from  $10^{-2}$  to 1, respectively.

The structural models [17,43,34,19] which are usually not appropriate for plastic foams due to possible modification of the skeleton's chemical formulation during the foaming processes and possible phase transitions are not studied here.

First, a brief recall of porous material mechanical behavior is presented. The methods are then described and classified into two classes: quasistatic methods where inertia effects are neglected and dynamic ones which are usually resonant. The advantages and drawbacks for each of these methods are presented and summarized at Section 4. This last section also addresses issues that still need to be solved.

In a second part, five of the methods described in the review are used to study the viscoelastic behavior of a melamine foam and to investigate the frequency and temperature dependences of its elastic parameters. Characterization results are compared and discussed.

## 2. Mechanical behavior

The understanding of porous materials' mechanical properties, in particular their viscoelastic ones and their symmetry groups (isotropy, transverse isotropy, orthotropy, etc.), is a prior step to their elastic and damping characterization.

In this paper, we mainly focus on polymer foams which usually exhibit a phase transition in the frequency and temperature domains of common use ([20–8000] Hz and [–50 to +50] °C). This phase transition is associated with a noticeable modification of the elastic and damping properties of the foams.

### 2.1. Viscoelasticity

The viscoelastic behavior of polymer foams is intermediate between the pure elastic solid state and the ideal viscous

liquid one. It thus results in a mechanical response depending on time. Moreover, the phenomena encountered with solid viscoelastic materials are also observed with porous materials having a polymer skeleton, namely (cf. [15]):

- if the stress is held constant, the strain increases with time (creep effect),
- if the strain is held constant, the stress decreases with time (relaxation effect),
- the effective stiffness depends on the rate of application of the load,
- if cyclic loading is applied, an hysteresis occurs leading to a dissipation of mechanical energy.

Fig. 1 illustrates the viscoelasticity behavior for the melamine foam presented at Fig. 3 when measuring the stress evolution versus strain for a constant strain rate deformation (the technique used to obtain the data is described at Section 3.2). Three regions can be identified on this figure [18]:

- Region 1: The linear bending region. In this region limited to small strains, the foam cells bend and stretch (the elastic parameters are measured in this region).
- Region 2: The buckling region. Stress increases slowly with strain due to the buckling of the foam cells.
- Region 3: The densification region. The cells collapse completely and the foam behaves as a solid material.

In the case of acoustical porous materials, which usually do not undergo large deformations for vibroacoustics purposes, studies in the literature are limited to the region of linear viscoelasticity. In this region, the Boltzmann's superposition principle (see [15] for example) which states that the total stress  $\sigma$  applied to a material is the sum of each stress  $\sigma_i$  generated by each deformation  $\varepsilon_i$ , is verified. The measurements presented here are carried out under this

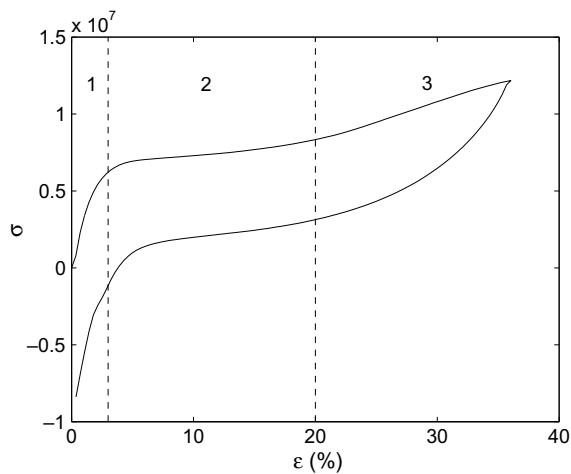


Fig. 1. Stress versus strain measurements for a melamine foam sample at 24 °C with constant strain rate deformation and recovery.

assumption of small deformations. Complex moduli are used to account for the viscoelastic behavior of acoustical porous materials submitted to time periodic loadings:

$$E = E'(\omega) + jE''(\omega) = E'(1 + j\eta(\omega)) \quad (1)$$

$$\text{with } \eta(\omega) = \frac{E''(\omega)}{E'(\omega)}. \quad (2)$$

In these equations,  $\omega$  is the angular frequency,  $j$  is the square root of  $-1$ .  $E'$  is the storage modulus which corresponds to a measure of the energy stored during a load cycle.  $E''$  is the loss modulus which represents a measure of the energy lost during the cycle.  $\eta(\omega)$  is the loss factor.

Note that for fibrous materials (and similar ones like felts), no linear zone is usually identifiable [14]. The range of strain values used during elastic characterization tests should thus be provided. Moreover, for these materials, Poisson's ratios are assumed to be equal to zero due to the weak or nonexistent links between the fibers (see [40] for example).

## 2.2. Anisotropy and inhomogeneity

Naturally, fibrous material are anisotropic from a mechanical point of view [41,40]. Foams are also subject to anisotropy due to gravity effects occurring during most of the foaming processes commonly used [18,4]. In particular, they may exhibit an orthotropic or transverse isotropy behavior [27], the foam cells being stretched in the foam expansion direction. However, despite these statements, few methods take this anisotropy into account.

In the following,  $E_i$  will refer to the Young's modulus of a material for direction  $i$ ,  $G_{ij}$  to the shear modulus for plane  $i-j$  and  $\nu_{ij}$  to the Poisson's ratio related to a strain in the direction of the second subscript resulting from a stress applied in the direction of the first subscript.

In addition to the anisotropy, a spatial inhomogeneity may also be observed especially for felts or materials composed of recycled products. To limit the potential effects of spatial heterogeneity the foam samples used in all tests presented in the second part (Section 5) have been cut off from the same small-sized block of material.

## 3. Descriptions of the methods

The methods described hereafter for the elastic and damping characterizations of acoustical foams have been classified into two classes: quasistatic methods and dynamic ones.

The quasistatic methods, for which the inertia effects are neglected, are valid for frequencies much smaller than the first resonance frequency of the system considered. A low coupling assumption between the material phases is also assumed in this regime. Porous materials are thus modeled as solid media. Three groups of quasistatic methods are identified according to their loading type: compression, torsion and pure shear (see respectively Sections 3.1–3.3).

The dynamic methods account for inertia effects and are thus valid at higher and usually wider frequency ranges. The descriptions of six groups of dynamic methods can be found respectively in Sections 3.4–3.9.

It is important to note that due to the amount of information, methods are only briefly described. The authors recommend to refer to cited articles to obtain exhaustive information about data acquisition and data processing for all the methods presented.

### 3.1. Brick under uniaxial compression loading, quasistatic regime

Fig. 2A presents the compression set-up described by Mariez et al. [26,27]: a cubic foam sample is placed between two parallel rigid planes. The lower plane is axially excited by an electrodynamic shaker while the higher plane is fixed. The planes are covered with sandpaper to avoid sliding of the sample against them; these boundary conditions allow to be close to clamped conditions without explicitly gluing the sample to the planes. The imposed deformation is of the form  $\varepsilon = \varepsilon_s + \varepsilon_d \sin(\omega t)$ , where  $t$  is the time variable,

$\varepsilon_s$  is the static strain fixed to avoid a surface inhomogeneity of the porous sample (which will be clearly observed for the melamine foam tested at Section 5.1),  $\varepsilon_d$  is the amplitude of a harmonic strain.

The elastic characterization is realized in two steps. First, the imposed displacement and an induced transverse displacement by Poisson's effect in a perpendicular direction are measured (by means of a laser vibrometer for this latter). This first step allows an estimation of this Poisson's ratio. Second, a measurement of the stiffness of the sample is done from the measured compression force and the imposed displacement. The complex Young's modulus, in the direction of the uniaxial compression,  $E$  is estimated by use of an inverse method based on precomputed results of a static three-dimensional solid finite element code (cf. [38] and [26,27]). The measurement operation can however be repeated changing the observation direction for the measurement of Poisson's ratios and the uniaxial compression direction to estimate the complex Young's moduli in the three-dimensional space.

An adaptation of this uniaxial compression test to cylindrical samples is proposed by Langlois et al. [25]. An isotropy of the material is assumed for this method based on charts from precomputed results to estimate the Young's modulus and Poisson's ratio from two material samples of different sizes.

In the case of fibrous materials (assuming their Poisson's ratios are equal to zero), Tarnov [40] proposed analytic expressions to estimate the complex Young's moduli from the experimental set-up described by [26,27].

### 3.2. Cylinder under torsion loading, quasistatic regime

One of the main interests of a torsion test compared to the previous uniaxial compression one is that it ensures a constant volume of the material during the loading. Consequently, the fluid–structure coupling can be considered to be lower for this method compared to previous compression tests.

The experimental set-up for this test, described at Fig. 2B, is quite similar to the uniaxial compression one except that one of the planes is harmonically excited in torsion and that the sample is of cylindrical shape. The shear stress and strain, obtained from measurements of a torque and an angular displacement transducers are used to calculate the complex shear modulus  $G$ . A more detailed description of this experimental set-up for which commercial devices exist is presented by Etchessahar et al. [14]. Section 5.2 shows the results obtained when applying this method to a melamine foam.

### 3.3. Layer under pure shear loading, quasistatic regime

The complex shear moduli of a material can also be estimated with a pure shear test. A complete description of a measurement set-up and an application to an open-cell polyurethane foam are presented in [14]. Two layers of the

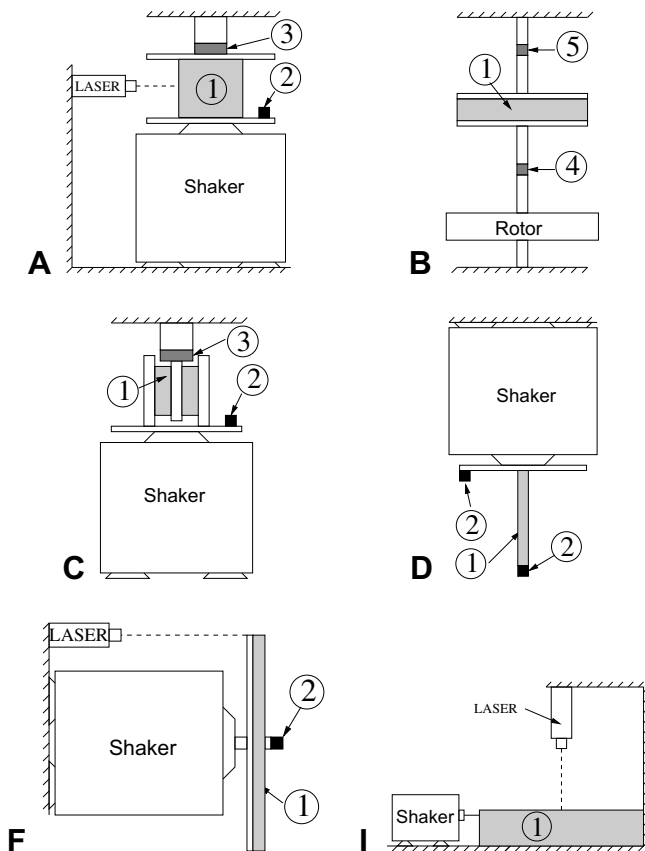


Fig. 2. Schematic representations of experimental set-ups for the elastic characterization of porous materials under various vibrating states or types of loading conditions and for different sample shapes. Vibrating state or load type A, uniaxial compression; B, torsion; C, pure shear; D, uniaxial traction-compression; F, point force; I, line force. 1, material sample; 2, accelerometer; 3, force transducer; 4, torque transducer; 5, angular displacement transducer. Set-ups are represented with a side view except for set-up F (top view).

material with identical dimensions are sandwiched between three parallel metal plates (cf Fig. 2C). The two external plates are connected to each other and are harmonically translated by a shaker. The vertical displacement,  $u$ , of these plates is measured by means of an accelerometer or an inductive displacement sensor. A force transducer placed between the top of the middle plate and the supporting frame is used to measure the transmitted force  $F$ . Finally, the complex shear modulus is estimated from the measured ratio  $F/u$  under the assumption that the thickness of the samples is small compared to its other dimensions.

An alternative measurement set-up involving only one material sample between two metal plates is presented in [40]. This last set-up is applied to estimate a complex shear modulus for a glass wool.

The above-illustrated quasistatic methods allow estimations of the elastic and damping properties of acoustical materials in frequency ranges that remain low compared to acoustical frequencies. Estimations at higher frequencies are possible with these set-ups from measurements at various temperatures and by making use of the frequency–temperature superposition principle [15,10] (an example of application of this principle will be presented in Section 5.2). However, as it will be concluded, it seems perilous to use the frequency–temperature superposition principle from measurements that consider only the solid phase of a diphasic material.

As an alternative to the use of the frequency–temperature superposition principle, the following section presents experimental methods for the dynamic evaluation of material parameters.

### 3.4. Beam under longitudinal vibrations

The complex Young's moduli  $E_i$  can be estimated from the modal analysis of a beam-like sample excited into longitudinal vibrations. The experimental set-up is depicted at Fig. 2D.

A first application to a close-cell foam was presented by Pritz [30]. The complex Young's modulus  $E$  is estimated from the analytical solution for resonance frequencies and resonance magnitudes of the one-dimensional wave equation. The porous material is considered as an "equivalent solid" in this basic modelling; displacements of the fluid phase are not accounted for in this model limited to a low frequency range (cf. [29]).

To minimize the influence of viscothermal effects, when applying this method to an open-cell material, Sfaoui proposes to realize measurements in vacuum [36,37]. It is at least recommended to test materials with very low or very high static air flow resistivities ([7,1]) and high densities to limit visco-inertial dissipative effects when measuring in air.

Another important point on which we will focus in the next sections is the fact that the material to adhesive layer interface is reduced to a minimum in this set-up.

Finally, this method presents the advantage to give a quick but rough (in the case of open-cell material) estima-

tion of  $E$  and its evolution with frequency in the approximate range [100–1000] Hz. Section 5.3 present the application of this method to a melamine foam.

### 3.5. Brick under uniaxial compression loading, dynamic regime

The quasistatic uniaxial compression test described at Fig. 2A and Section 3.1 can be adapted to a mass-spring system [11]. The fixed plane is replaced by a mass with a known weight. The estimations of the elastic parameters for the material under test is realized by studying the first mass-spring resonance of the system. First, the dynamic stiffness of the material sample at the resonance frequency is computed then the complex Young's modulus in the direction of the uniaxial compression is deduced using the same computational technique as the one described for the quasistatic method 2A. From measurements on two samples of different dimensions, an estimation of the Poisson's ratio can also be done (the material is still supposed to be isotropic).

Caution should be taken in the choice of the sample as the mass may rotate in the case of a non-homogeneous material. This phenomenon leads to the excitation of other vibrational modes with eigenfrequencies which may be close to the mass-spring mode one. This usually results in unreliable characterizations. An interesting study on this topic, and moreover applied to a melamine foam, is presented by Guastavino et al. in [21].

### 3.6. Beam under bending vibrations

A beam sample can also be tested under bending vibrations as described in the set-up F of Fig. 2 [45]. In this method, which derived from the Oberst's beam method [5], a shaker is set at the center of a base metal beam supporting the foam layer and imposes a transverse displacement. A laser vibrometer measures the transverse velocity of the base beam at one free tip.

The determination of the material Young's modulus and the loss factor in the direction of the beam axis is carried out with an inverse calculation. However, to observe a significant modification in the vibration behavior of the metal base beam, the material thickness should overcome the Ross Kerwin and Ungar's model assumptions [33], numerical computations are then required.

In the case of very low Young's modulus to measure (typically less than  $10^6 \text{ N m}^{-2}$ ) a constrained metal beam can be added on top of the foam layer as described in the original Oberst's method. The vibration behavior is then mainly due to shear strain of the sample material under test. Numerical computations are also required to inverse the material modulus in this case.

One advantage of this method is to allow a diphasic modelling of the porous medium. The main disadvantage of this method is the heavy computational resources required. The method presented in the following section

attempts to solve this problem by using a simplified calculus to model a plate-porous configuration.

### 3.7. Plate under bending vibrations

Etchessahar et al. [13] have proposed to study the vibrations of a standalone clamped porous plate to estimate the elastic and damping parameters of the material. A fit of Prony series [39] is proposed to identify the parameters at resonance frequencies. However, the experimental difficulty faced for applying a point force on the porous medium lead Etchessahar and colleagues to conclude that a two-layer configuration should be of greater interest.

Jaouen et al. have presented such a configuration in [24]. A layer of porous material is bonded onto a metal plate. A shaker imposes a transverse point load on this base metal plate. The input force on the plate is measured by means of a force transducer and its transverse velocity is measured by a laser vibrometer or by the integration of a light accelerometer signal.

A simplified model, based on the mixed displacement–pressure formulation of the Biot–Allard theory [6] is used to predict the vibration behavior of this composite plate at low frequencies (for the first resonance frequencies). The base plate and the porous solid phase are described as an equivalent viscoelastic plate; the fluid phase and its coupling with the solid one is also accounted for. The poroelastic layer is assumed to be isotropic.

A non-linear inversion algorithm is then used to estimate the Young's modulus and the loss factor at the system resonance frequencies from the measurements and numerical simulations. The Poisson's ratio is assumed to be equal to its quasistatic value obtained from a quasistatic method such as method 3.1.

The results of this method applied to a melamine foam are reported at Section 5.5.

### 3.8. Acoustical excitation-based methods

Methods based on acoustical excitations of material samples have also been proposed. Most take advantage of the first quarter wavelength resonance in the thickness of a porous layer glued to a rigid backing.

Sellen [35] has proposed estimations of the Young modulus, the loss factor and Poisson's ratio of a material by fitting surface impedance and sound absorption measurements in a standing wave tube with simulation results from a complete isotropic poroelastic model. The exact circumferential boundary conditions of the sample in the tube which largely influence the results [42,28], is the main drawback of this method which can give, with confidence, orders of magnitude for the elastic parameters.

In the same time, Garetton et al. [16] presented a method based on the normal acoustic surface impedance measurement of a large and thick material sample backed by a rigid wall and loaded with a solid plate in free sound pressure field generated by a sound pressure monopole.

Allard et al. [2] have modified this last set-up to estimate one shear modulus of a thin porous sample (with a thickness around 5 or 10 mm) from the localization of a pole of the reflection coefficient at oblique incidence, near the grazing incidence. The estimations of the shear modulus relies on the fitting of a curve and the assumption that the corresponding Poisson's ratio is real and constant with the frequency.

These last two works and the theoretical developments realized to describe the propagation of surface waves on porous material have opened new perspectives for the elastic characterization of porous materials.

### 3.9. Phase velocity measurement-based methods

Allard et al. [3] proposed in 2002 a method for the estimation of one shear modulus from the study of the Rayleigh structure borne surface wave on a porous material. Despite this method has the inconvenience, like most of the acoustic ones previously presented, to require large samples, it allows estimations of an elastic modulus at frequencies higher than the usual methods: from 2 to 4 kHz. This method has, later on, been extended to lower frequencies or thinner samples [8].

In 2005, Boeckx et al. [9] also presented a method allowing the estimation of a complex shear modulus and a complex Poisson's ratio in the approximate frequency range 200–1300 Hz. Fig. 2I is a schematic representation of the experimental set-up. The bottom side and an end of a large and thick sample layer is glued with a double sided tape to a rigid metal plate. The opposite end is excited with varying frequencies on its width by a thin metal strip attached to a shaker so that the entire edge is excited simultaneously. The vertical displacements in the harmonic regime induced by the excitation on the free upper side of the sample are measured with a laser vibrometer along a line from the excited end to the motionless one. Spatial Fourier transforms of these displacement profiles are computed to deduce the wave numbers and phase velocities. The shear modulus, its corresponding loss factor and a Poisson's ratio are then estimated by fitting the measurements phase velocities with results from a theoretical model.

## 4. Summary and discussion

Table 1 summarizes the frequency ranges, temperature ranges and sample sizes usually observed for the methods presented. Temperature ranges may be limited by the transducers used. In particular, shakers and accelerometers have usually a narrow temperature range of use.

Table 2 adds comments on the methods and recalls their main advantages or drawbacks.

From the analysis of Tables 1 and 2, it is obvious that no unique method can be applied to estimate accurately the elastic and damping parameters of all existing acoustical porous material. Moreover, a number of issues needing attention can be listed.

Table 1  
Method groups, approximate frequency and temperature ranges of use, sample shape and size

| Method group | Description                                    | Freq. range (approximate, Hz) | Temp. range (approx., °C) | Sample shape and size   |
|--------------|--|-------------------------------|---------------------------|---|
| A, E         | Uniaxial compression (quasistatic and dynamic) | 1–100                         | 0 to +40                  | Brick or cylinder; at least ~20 mm thick, 40 mm thick recommended |
| B            | Torsion  | $10^{-2}$ to 10               | 0 to +40                  | Cylinder, at least ~10 mm thick                                   |
| C            | Pure shear                                     | $10^{-2}$ to 10               | 0 to +40                  | Parallelepipedic of few cm long and few mm thick                  |
| D            | Longitudinal                                   | 100–1000                      | 0 to +40                  | Beam, length of 200 mm at least                                   |
| F, G         | Beam, plate bending                            | 100–1000                      | 0 to +40                  | Beam or plate, one side of at least 400 mm long                   |
| H            | 1/4 wavelength resonance                       | 100–1000                      | Ambient                   | Plate, surface of 1 m <sup>2</sup> at least                       |
| I            | Phase velocity (general)                       | 100–1000                      | Ambient                   | Surface of 1 m <sup>2</sup> at least                              |
|              | Rayleigh wave                                  | $10^3$ – $10^4$               |                           | Thick sample  |

Table 2  
Method groups, comments on use

| Method group | Description                                    | Comment   |
|--------------|--|---|
| A, E         | Uniaxial compression (quasistatic and dynamic) | Allow direct measurement of Poisson's ratios. Method described by Mariez et al. allows characterization of orthotropic materials (under some assumptions) |
| B            | Torsion  | Commercial devices widely spread. Fluid phase effects are limited, simple and fast modelling available  |
| C            | Pure shear                                     | Simple and fast modelling available   |
| D            | Longitudinal                                   | Simple and fast modelling available   |
| F, G         | Beam, plate bending                            | Time and memory consuming inversion methods unless use of dedicated numerical codes   |
| H            | 1/4 wavelength resonance                       | Sensitive to boundary conditions  |
| I            | Phase velocity                                 | Rayleigh wave method allow estimation in approximate freq. range from 2 to 4 kHz  |

- Most of the dynamic methods are based on a major, and wrong, assumption assuming Poisson's ratios  $\nu_i$  are real and constant in each frequency range of measurement. This assumption was first invoked due to the difficulties faced when trying to directly measure Poisson's ratios. The evaluation of a Poisson's ratio from estimations of two moduli [31] appears as a simpler solution than a direct measurement of this Poisson's ratio.
- It has been shown that the fluid phase has an influence on the estimations of the elastic parameters even for quasistatic methods [12,11]. The influence of acoustical properties uncertainties for the dynamic evaluations of elastic and damping properties of porous materials is currently investigated but still remains a widely open question. In a more general way, the uncertainties on the elastic parameter estimations are usually not reported.
- In the case of multi-layered configurations using a base beam or a base plate, the exact condition at the metal-porous interface is not exactly known. A perfect bond is always supposed in the modelling and the influence of the gluing conditions are rarely investigated although their influence on the characterization results may not be negligible [23,45].
- Finally, too less work has been done to consider the anisotropy of acoustical porous materials yet.

In conclusion to this part, the safest way to characterize a porous material is to use a combination of methods

according to their limitations and in connection with the sizes of the available material samples.

## 5. Application to a melamine foam

In order to test the robustness of some of the previously presented methods, five of them are used to estimate the Young's or shear moduli and loss factors of a melamine foam. This lightweight, heat and flame resistant, open-cell material is used, or can be potentially used, for sound absorption or sound insulation in the fields of building construction and transportation. Melamine foams are used in wedges of anechoic rooms or inside fuselages of airplanes.

The choice of a melamine foam was guided by the fact the manufacture process for this material is well controlled and that it possesses interesting elastic properties to illustrate the methods presented in the first part of this article. Moreover, samples can be cut easily from this material.

Fig. 3 shows a picture of the cell morphology for this material.

In the following, the same perpendicular directions (or axes) 1, 2 and 3 will be used to orientate all foam samples; subscripts 1, 2 and 3 will refer to a quantity measured or estimated in one of these directions. These samples have all been cut off from a small-sized block of melamine foam to avoid spatial heterogeneity as much as possible.

Note that an interesting study of the heterogeneity and anisotropy of this material has been published recently by Guastavino et al. [20,21].

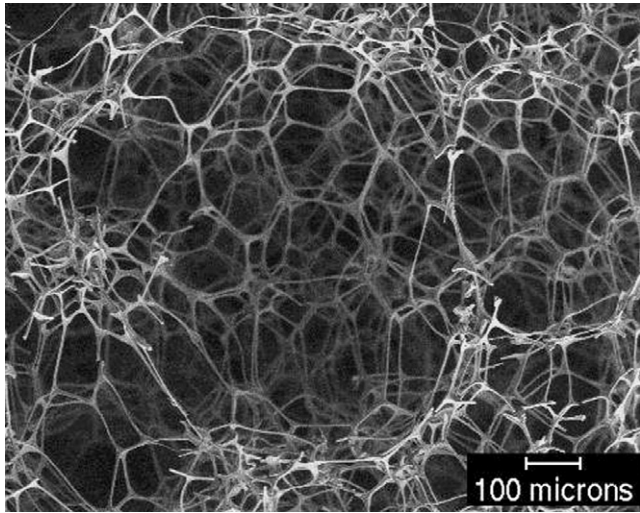


Fig. 3. Electron microscope picture of the tested melamine foam. The solid phase, or skeleton, of the foam appears in white.

5.1. Brick under compression loading, quasistatic regime

The method described at Section 3.1 has been applied to a  $40 \times 40 \times 40 \text{ mm}^3$  sample of the melamine foam (more precisely, the method used here is the one described by Mariez et al. [26]). Fig. 4 shows the variations of the Young's modulus  $E_3$  and the loss factor  $\eta_3$  with the static strain  $\epsilon_s$ .

The linear domain of measurement for the elastic properties is obtained for a static strain  $\epsilon_s$  equal to 2% (the thickness of the surface inhomogeneities are thus estimated around 0.8 mm).

Estimation results for the Young's moduli  $E_i$  and loss factors  $\eta_i$  at 18 °C for the three perpendicular directions 1, 2 and 3 of the same sample of melamine foam are presented at Fig. 5. These values confirm the elastic anisotropy of the melamine foam and, more precisely, that this material has a symmetry close to an orthotropic one (assuming

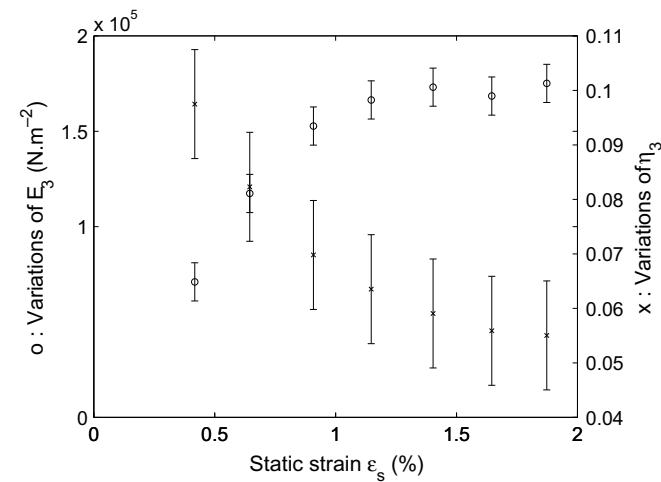


Fig. 4. Compression test on direction 3 of a melamine foam cubic sample ( $40 \times 40 \times 40 \text{ mm}^3$ ) at 18 °C. Error-bars are computed from measurement uncertainties.

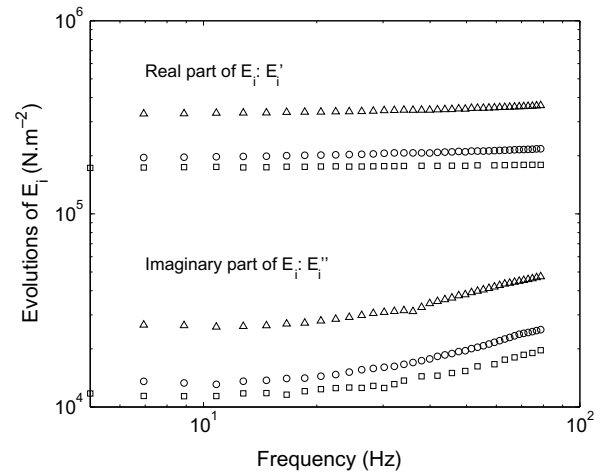


Fig. 5. Estimation of the melamine foam complex Young's moduli at 18 °C. Test in compression [26,27]. (○) Direction 1, (△) direction 2, (□) direction 3.

the principal axis of the material are parallel to the cube directions 1, 2 and 3). The accuracy of the results obtained for such an isotropic material with this method, based on a isotropic model, will be discussed in Section 5.6.

Another remarkable point is the increase of the moduli with frequency which confirms the viscoelastic behavior of the foam. Values over 70 Hz are reported although the low coupling effects assumption between the material phases for this foam and this configuration is no more valid above this frequency [12,11].

Fig. 6 shows measurement results for the Poisson's ratio  $\nu_{23}$  in the frequency range [40–80]. This frequency range differs from the one used for the measurements of Young's moduli, the sensors used was different and the authors were not able to have consistent values for the Poisson's ratio below 40 Hz. These Measurements of the Poisson's ratio  $\nu_{23}$  show slow decreases of its real and imaginary parts with the frequency. These observations are coherent with the theory of viscoelasticity presented at Section 2. In first

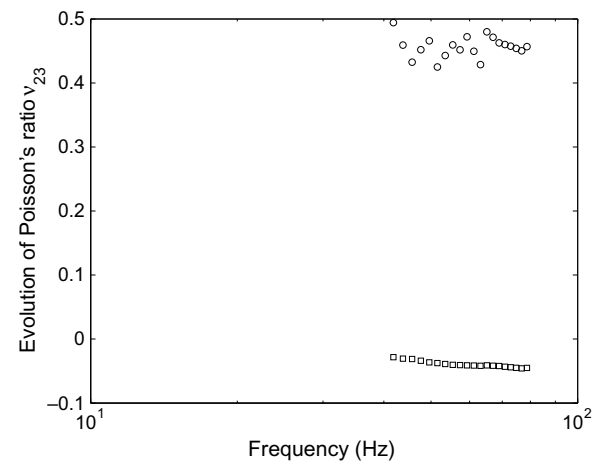


Fig. 6. Evolution of the complex Poisson's ratio  $\nu_{23}$  at 18 °C. Test in compression [26,27]. (○) Real part, (□) imaginary part.



approximation, this Poisson’s ratio can however be considered as real (the imaginary part having values very close to 0) and constant. This approximation, limited to a narrow frequency range, has been extensively used by the past [26,27,25,45,2,8] under valid conditions and less valid ones (because applied to a wider or different frequency range than the measurements one). Under this real and constant approximation,  $\nu_{23}$  is found to be equal to 0.44, its mean value over the measurement data for its real part. This value is close to the one obtained in the same frequency range by the authors from the version of this experimental set-up adapted to cylindrical shaped [25]: 0.45.

5.2. Cylinder under torsion loading, quasistatic regime

Measurements for the melamine foam, at temperatures from 0 to 40 °C, with a commercial Rheometric Scientific RDA II apparatus are reported in Figs. 7 and 8 (Fig. 1 is also plotted from measurements obtained with this apparatus). Radius and height of the cylindrical samples used are 31 and 10 mm, respectively.

One can note that the order of magnitude for the complex shear modulus  $G_{23}$  at 24 °C and 2 Hz, for example, is coherent with the order of magnitude of the complex Young’s moduli estimated with the quasistatic compression test at 18 °C and 7 Hz. This point allows a first consistency check of the measurements remembering that for viscoelastic materials, the frequency dependences of the complex shear moduli and the complex Young’s moduli are alike.

In addition, a state transition is clearly observed at 24 °C, on Fig. 8, in the [0.01–10] Hz frequency range. However, without any additional information, no conclusion can be made on the nature of this transition.

An example of application of the frequency–temperature superposition principle from measurement results of Figs. 7 and 8 is shown at Fig. 9. The variations of the real and imaginary parts of  $G_{23}$  are estimated for a temperature of 24°.

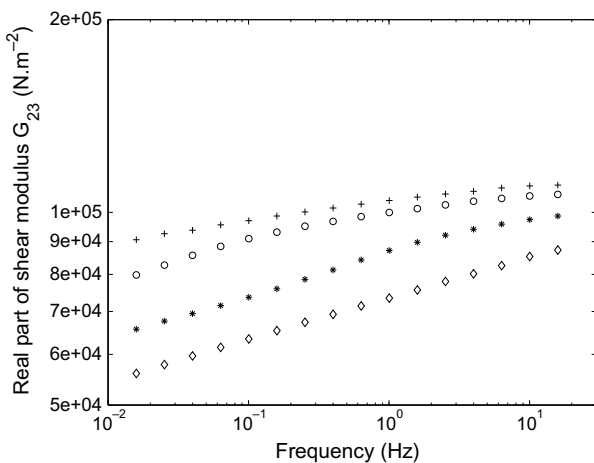


Fig. 7. Variations of the shear modulus real part  $G'_{23}$  with temperature and frequency for the melamine foam. (+) 0, (O) 10, (\*), (◇) 24, (◇) 40 °C.

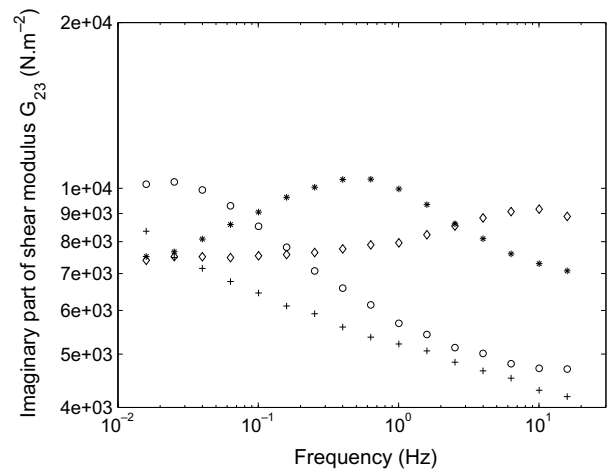


Fig. 8. Variations of the shear modulus imaginary part  $G''_{23}$  with temperature and frequency for the melamine foam. (+) 0, (O) 10, (\*), (◇) 24, (◇) 40 °C.

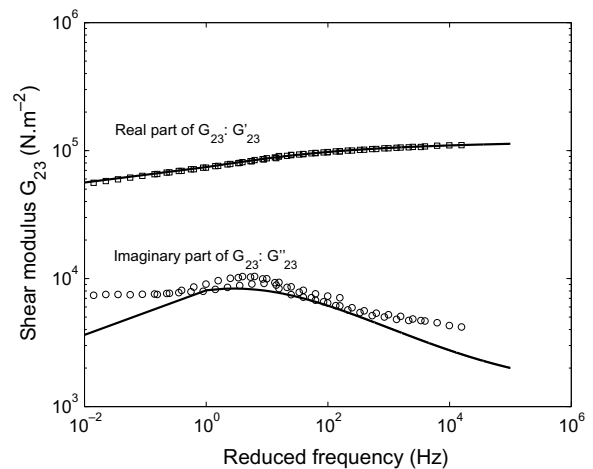


Fig. 9. Real and imaginary parts of complex modulus  $G_{23}$ :  $G'_{23}$ ,  $G''_{23}$  for melamine foam at 24 °C. (O) Points from measurements, (solid line) five parameters viscoelastic model described in [32].

This frequency–temperature superposition representation has been obtained from horizontal shifts of the measured real part of  $G_{23}$  at various temperatures. Coefficients of the Williams–Landel–Ferry equation [44], computed from a least square fit of the horizontal shifts values, are:  $C_1 = 7.23$  and  $C_2 = 98.42$ .

One can observe a good correspondance between the real part of the modulus  $G_{23}$  and the linear model of viscoelasticity introduced by Pritz [32] (Zener derivative model) with fitted parameters:  $G_0 = 49,300 \text{ N m}^{-2}$ ,  $d = 2.16$ ,  $\alpha = 0.350$ ,  $\beta = 0.338$  and  $\tau = 0.084$  (using the same notation as in [32]).

The frequency–temperature superposition applied to the loss modulus  $G''_{23}$  results in much more scattered data. The difficulty to estimate precisely high loss factor values as those encountered for acoustical porous material (usually around 0.1) explained partly this fact.

One can also observed a bias between the measurements and the application of the linear model of viscoelasticity: values of the loss modulus are overestimated in the whole frequency range studied. Again, the difficulty to estimate precisely high loss factor values explained partly this fact. Moreover, the influence of the fluid phase and its coupling to the solid one, neglected in the model used, may add to the previous difficulty. This influence, mainly of visco-dissipative nature, is supposed to remain small at low frequencies [11] but may differ with the temperature. It thus appears perilous to use the frequency–temperature superposition principle from measurements that consider only the solid phase of a diphasic foam.

5.3. Beam under longitudinal vibrations

Figs. 10 and 11 show the results obtained with this method applied to a 185 mm wide and  $10 \times 10 \text{ mm}^2$  cross-section melamine foam beam as circle marks.

Although the melamine foam is an open cell material, this method gives coherent results with the theory of viscoelasticity, for the first two modes. The model used in [30], which does not account for the material fluid phase, shows its limitations with increasing frequency when the fluid phase and its coupling with the solid phase are not negligible [12,11]. A more general model of open-cell porous media, as the Biot–Johnson–Champoux–Allard’s [7,1] model is thus needed to account for the inertial, viscous and thermal interactions between the material two phases and their effects on the vibration response of the sample.

Results from this method are discussed further and compared with those obtained from the two following methods at Section 5.6.

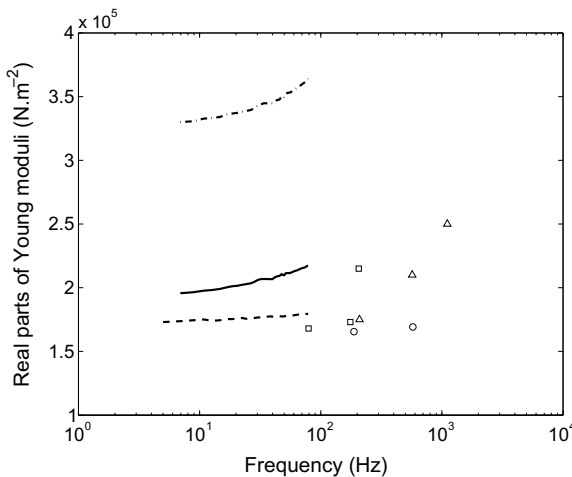


Fig. 10. Comparison of the results obtained for the Young’s moduli of melamine foam. Solid, dashed–dotted and dashed curves: quasistatic compression test 2A at 18 °C for directions 1, 2 and 3, respectively; (○) beam under longitudinal vibrations (set-up 2D, dir. 1, 25 °C), (□) plate under bending vibrations (method described at Section 3.7, dir. 1 and 3, 23 °C), (△) beam under bending vibrations (set-up 2F, dir. 1, 20 °C).

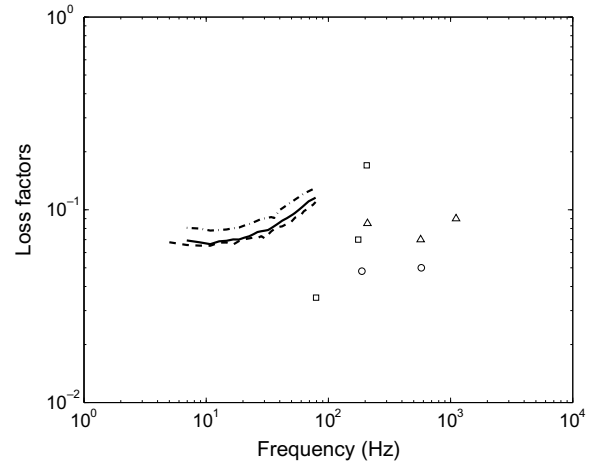


Fig. 11. Comparison of the results obtained for the loss factors of melamine foam. Solid, dashed–dotted and dashed curves: quasistatic compression test 2A at 18 °C for direction 1, 2 and 3, respectively; (○) beam under longitudinal vibrations (set-up 2D, dir. 1, 25 °C), (□) plate under bending vibrations (dir. 1 and 3, 23 °C), (△) beam under bending vibrations (set-up 2F, dir. 1, 20 °C).

5.4. Beam under bending vibrations

Figs. 10 and 11 show results of this method applied to the melamine foam at a temperature of 20 °C as triangular marks.

Measurements have been realized at six temperatures from 5 to 30 °C (by steps of 5 °C), but the low evolution of the elastic parameters for this foam does not allow an extrapolation to a noticeably wider frequency range using the frequency–temperature superposition principle.

Indeed, one can observe that the results shown at Figs. 10 and 11 for temperature of 20 °C are close to those obtained from the quasistatic compression test at 18 °C (cf. Section 5.1) for direction 1. One also notices that the real part of the modulus increases with the frequency at a fixed temperature thus confirming the consistency of the results.

5.5. Plate under bending vibrations

The results of this method applied to the melamine foam at a temperature of 20 °C are reported in Figs. 10 and 11 as square marks. The aluminum base plate used had size of  $520 \times 560 \times 3.175 \text{ mm}^3$  and the foam sample was 25.4 mm thick.

5.6. Comparison of the results

A good correspondence is observed between the results of Figs. 10 and 11 obtained from the different methods. The evolutions of the moduli are coherent with the theory of viscoelasticity (moduli increase with the frequency at a given temperature). Moreover, the estimations for a same direction are of the same order of magnitude and in addition, these estimations are close one to each other. These

results, originally published in [23], are also found to be concordant with those presented in [9] at a temperature around 21 °C.

However, two remarks on these results can be made. First, in the upper frequency range of use of most methods, the increase of the elastic moduli, and loss factors, seem too important to be trustworthy. Several reasons can be invoked to explain this observation among which are the following.

- The effects of the fluid phase may not be negligible as supposed in the modelling for methods of groups A and B.
- Methods of group A are based on a biased model which assumes the material is isotropic even if it has been previously reported in this article that this is not the case for the tested porous medium. Nevertheless, it can be observed that the estimation obtained for Young's modulus  $E'_1$  with such a method are close to estimations obtained from others set-ups and in particular the ones based on a one-dimensional model.
- Methods in groups A, F and G which are based on numerical computations can be subjected to a lack of convergence during the inversion process leading to approximative values of the elastic parameters.

The second remark is that the loss factor results are much more scattered than those for the real parts of the Young's moduli. This observation illustrates the experimental difficulty to estimate high loss factors. The lowest values might be representative of the foam's loss factors while higher values might be related to model or methods inconsistency as discussed in the previous paragraph.

In the case of direction 1, estimations of the deviations between the different methods for the real Young's modulus  $E'_1$  and its corresponding loss factor  $\eta_1$  can be computed. Around 200 Hz, the mean value and standard deviation of  $E'_1$  (computed over the three methods giving results around this frequency: beam under longitudinal or bending vibrations and plate under bending vibrations) are  $1.80 \times 10^5$  and  $0.25 \times 10^5$  Pa approximately. The relative error for the estimation of  $E'_1$  can thus be estimated to 14% approximately. This error is acceptable compared to the error usually observed when estimating a real elastic modulus for a solid material. Concerning the loss factor  $\eta_1$ , its mean value and standard deviation are 0.10 and 0.06 approximately. The relative error is thus computed to 60% approximately.

## 6. Conclusion

Available experimental methods for the elastic and damping characterization of acoustical porous materials have been presented after a brief recall of the mechanical behavior (viscoelastic, anisotropic and inhomogeneous) of these materials, in particular polymer foams and fibrous materials.

The methods have been categorized in two classes (quasistatic and dynamic methods) or nine groups depend-

ing on the vibrating states or load types. The main advantages and drawbacks of each method have been discussed individually and a number of general issues has been reported. These points requiring attention are: (i) an usual and wrong assumption of real and constant Poisson's ratios in a large frequency band, (ii) the non-negligible influence of the fluid phase even at low frequencies – around 100 Hz and more; (iii) the effects of the gluing layer between the apparatus and the material sample rarely accounted for, (iv) too less work has been done to consider anisotropy of the materials.

Finally, five of these methods have been applied to a melamine foam to investigate the frequency and temperature dependences of its elastic parameters. The deviations between the results obtained from the different tested methods have been reported. These values cannot be generalized to other materials but give a first estimation of the parameters accuracy. Inter-laboratory tests may also be carried out on more materials to have a better evaluation of the bias and error of each characterization method.

## Acknowledgements

The authors thank F. Paris for helping them to obtain the electron microscope picture reproduced at Fig. 3, L. Benyahia for the torsion test results, F.-X. Bécot and reviewers of the manuscript for their valuable comments.

## References

- [1] Allard J-F. Propagation of sound in porous media. Modeling sound absorbing materials. Amsterdam: Elsevier; 1993.
- [2] Allard J-F, Henry M, Boeckx L, Leclaire P, Lauriks W. Acoustical measurement of the shear modulus for thin porous layers. *J Acoust Soc Am* 2005;117:1737–43.
- [3] Allard J-F, Jansens G, Vermeir G, Lauriks W. Frame-borne surface waves in air-saturated porous media. *J Acoust Soc Am* 2002;111:690–6.
- [4] Ashby MF, Evans A, Fleck NA, Gibson LJ, Hutchinson JW, Wadley HNG. *Metal Foams: a design guide*. London: Butterworth Heine- mann; 2002.
- [5] ASTM E756-98. Standard test method for measuring vibration-damping properties of materials. American Society for Testing and Materials, 1998.
- [6] Atalla N, Panneton R, Debergue P. A mixed displacement–pressure formulation for poroelastic materials. *J Acoust Soc Am* 1998;104(3):1444–52.
- [7] Biot MA. Theory of deformation of a porous viscoelastic anisotropic solid. *J Appl Phys* 1956;27:459–67.
- [8] Boeckx L, Leclaire P, Khurana P, Glorieux C, Lauriks W, Allard J-F. Guided elastic waves in porous materials saturated by air under lamb conditions. *J Appl Phys* 2005;97:094911.
- [9] Boeckx L, Leclaire P, Khurana P, Glorieux C, Lauriks W, Allard J-F. Investigation of the phase velocities of guided acoustic waves in soft porous layers. *J Acoust Soc Am* 2005;117:545–54.
- [10] Corsaro RD, Sperling LH, editors. Sound and vibration damping with polymers. In: *ACS symposium series 424*. Washington (DC): American Chemical Society; 1990.
- [11] Danilov O, Sgard F, Olny X. On the limits of an “in vacuum” model to determine the mechanical parameters of isotropic poroelastic materials. *J Sound Vib* 2004;276:729–54.

- [12] Dauchez N, Etchessahar M, Sahraoui S. On measurement of mechanical properties of sound absorbing materials. In: Poromechanics II. Proceedings of the 2nd Biot Conference, 2002, p. 627–31.
- [13] Etchessahar M. *Caractérisation mécanique en basses fréquences des matériaux acoustiques*. PhD thesis, Université du Maine, Le Mans, France, 2002.
- [14] Etchessahar M, Benyahia L, Sahraoui S, Tassin J-F. Frequency dependence of elastic properties of acoustics foams. *J Acoust Soc Am* 2005;117:1114–21.
- [15] Ferry JD. *Viscoelastic properties of polymers*. New York: Wiley; 1961.
- [16] Gareton V, Etchessahar M, Lafarge D, Sahraoui S. Comparaison d'une méthode mécanique et d'une méthode acoustique pour la caractérisation des mousses de polyuréthane. In: CDROM of the Proceedings of the Sixth Congrès Français d'Acoustique, Lille, 2002.
- [17] Gent AN, Thomas AG. Mechanics of foamed elastic materials. *Rubber Chem Technol* 1963;36:597–610.
- [18] Gibson LJ, Ashby MF. *Cellular solids: structure and properties*. Oxford: Pergamon Press; 1988.
- [19] Gong L, Kyriakides S, Jang W-Y. Compressive response of open-cell foams. Part I: Morphology and elastic properties. *Int J Solids Struct* 2005;42:1355–79.
- [20] Guastavino R. Elastic and acoustic characterisation of porous layered system. PhD thesis, Thesis for the licenciate degree of engineering, KTH, Stockholm, ISSN 1651-7660, 2006.
- [21] Guastavino R, Göransson P, Hörlin N-E. Characterisation of anisotropic porous foam materials. In: CDROM of the Proceedings of the First Symposium of the Acoustics of Poro-Elastic Materials, ENTPE, Lyon, France, 2005.
- [22] Hilyard NC, Cunningham A. *Low density cellular plastics, physical basis of behaviour*. London: Chapman & Hall; 1994.
- [23] Jaouen L. *Contribution à la caractérisation mécanique de matériaux poro-visco-élastiques en vibro-acoustique*. PhD thesis, Université de Sherbrooke (Canada), Université du Maine (Le Mans, France), 2003.
- [24] Jaouen L, Brouard B, Atalla N, Langlois C. A simplified numerical model for a plate backed by a thin foam layer in the low frequency range. *J Sound Vib* 2005;280(3–5):681–98.
- [25] Langlois C, Panneton R, Atalla N. Polynomial relations for quasi-static mechanical characterization of isotropic poroelastic materials. *J Acoust Soc Am* 2001;110:3032–40.
- [26] Mariez E, Sahraoui S, Allard J-F. Elastic constants of polyurethane foam's skeleton for the Biot model. In: Proceedings of Internoise, Liverpool, 1996. p. 951–54.
- [27] Melon M, Mariez M, Ayrault C, Sahraoui. Acoustical and mechanical characterization of anisotropic open-cell foam. *J Acoust Soc Am* 1998;104:2622–7.
- [28] Pilon D, Panneton P, Sgard F. Behavioral criterion quantifying the edge-constrained effects on foams in the standing wave tube. *J Acoust Soc Am* 2003;114:1980–7.
- [29] Pilon D, Panneton R. An equivalent solid (u) formulation for poroelastic materials. In: Proceedings of the 144th ASA meeting, Cancun, 2002.
- [30] Pritz T. Dynamic Young's modulus and loss factor of plastic foams for impact sound isolation. *J Sound Vib* 1994;178:315–22.
- [31] Pritz T. Frequency dependences of complex moduli and complex Poisson's ratio of real solid materials. *J Sound Vib* 1998;214:83–104.
- [32] Pritz T. Five-parameter fractional derivative model for polymeric damping materials. *J Sound Vib* 2003;265(5):935–52.
- [33] Ross R, Ungar EE, Kerwin EM. Damping of plate flexural vibrations by means of viscoelastic laminate, structural damping. In: Proceedings of ASME, Struct. Damping Sec. (3), New York, 1959, p. 49–88.
- [34] Sahraoui S, Mariez E, Etchessahar M. Linear elastic properties of anisotropic open-cell foams. *J Acoust Soc Am* 2001;110:635–7.
- [35] Sellen N. Modification de l'impédance de surface d'un matériau par contrôle actif: application à la caractérisation et l'optimisation d'un absorbant acoustique. PhD thesis, Ecole Centrale de Lyon, France, 2003.
- [36] Sfaoui A. On the viscoelasticity of the polyurethane foam. *J Acoust Soc Am* 1995;97:1045–52.
- [37] Sfaoui A. Erratum: on the viscoelasticity of the polyurethane foam. *J Acoust Soc Am* 1998;98:665.
- [38] Sim S, Kim K-J. A method to determine the complex modulus and Poisson's ratio of viscoelastic materials from FEM applications. *J Sound Vib* 1990;141(1):71–82.
- [39] Simo JC, Hugues TRJ. *Computational inelasticity*. Berlin: Springer; 1998.
- [40] Tarnow V. Dynamic measurements of the elastic constants of glass wool. *J Acoust Soc Am* 2005;118(6):3672–8.
- [41] Tran-Van J, Olny X. Mechanic properties of transverse isotropic porous materials, effect on sound transmission in double lightweight walls: theoretical approach. In: CDROM of the Proceedings of Internoise, Prague, 2004.
- [42] Vigran TE, Kelders L, Lauriks W, Leclaire Ph, Johansen TF. Prediction and measurements of the influence of boundary conditions in a standing wave tube. *Acta Acust* 1997;83:419–23.
- [43] Warren WE, Kraynik AM. The linear elastic properties of open-cell foams. *J Appl Mech* 1988;55:341–6.
- [44] Williams ML, Landel RF, Ferry JD. Temperature dependence of relaxation mechanisms in amorphous polymers and other glass-forming liquids. *J Am Chem Soc* 1955;77:3701–6.
- [45] Wojtowicki J-L, Jaouen L, Panneton R. A new approach for the measurement of damping properties of materials using the Oberst beam. *Rev Sci Instrum* 2004;75(8):2569–74.